Energy limitation for models to simulate the buffer gas cooling

Z.C. Zhu[a,b], W.X. Huang[*,a], Y.L. Sun[a,b], Y. Wang[a], Y.L. Tian[a], J.Y. Wang[a]

[a]*Institute of Modern Physics, Chinese Academy of Sciences, Lanzhou 730000, China*
[b]*Graduate University of Chinese Academy of Sciences, Beijing 100049, China*

Abstract

Detailed simulations of buffer gas cooling, which is widely applied at the rare-isotope facilities, have been investigated by using three frequently used models: viscous damping force (VDF) model, hard sphere collision (HSC) model, and realistic interaction potential (RIP) model. By comparing the stopping ranges from the simulated data with those from SRIM code, we found that the VDF and HSC models are better in low energy range, but the RIP model is better in relatively high energy range. In helium buffer gas, which is always used in cooler and bunchers, the VDF model should be used when the ion's energy is less than ~ 5 eV/u, and the RIP model less than ~ 80 eV/u. Above this energy, all three models can not be used.

Key words: Ion trap, Ion cooling, Buffer gas cooling, Stopping power
PACS: 29.27.Eg, 41.75.-i, 41.85.Ct, 34.50.Bw

[*]Corresponding author.
Email addresses: zhuzhichao@impcas.ac.cn (Z.C. Zhu), huangwx@impcas.ac.cn (W.X. Huang)

1. Introduction

Buffer gas cooling is widely applied at the rare-isotope facilities nowadays [1–4]. By combining with radiofrequency ion guide, the continuous ion beams can be improved and the cooled ion bunches with low emittance and small spread can be provided. This method is universally applicable to all elements ranging from helium to the heaviest elements [5], and is rather fast that the ions could be cooled within single pass through the cooler device. It has become one of the essential parts for the successfully high-precision Penning trap mass measurements.

In order to obtain the high performance of ion beam cooler, detailed simulation of buffer gas cooling is critical. There are three models frequently used for such a simulation: viscous damping force (VDF) model, hard sphere collision (HSC) model, and realistic interaction potential (RIP) model. VDF model is a macroscopic approach by providing a simple prescription of the time-averaged cooling force, and the others are microscopic methods by tracking the cooling process by simulating individual collision between the ion and the buffer gas molecule.

The buffer gas cooling effect has been simulated by many researchers. Lunney and Moore [6] developed a simulation package to simulate a radio frequency quadrupole rod system operated in helium buffer gas for cooling ion beam to reduce its emittance. Results indicated that an emittance reduction of almost 2 orders of magnitude in all coordinates was possible with near 100% transmission barring charge exchange and molecular formation.

Kim [7] used both the HSC and RIP models to simulate the cooling process of ions in a gas-filled ion guide and to compare the calculated tem-

2

perature of cooled ions to experimental data. Only the calculations with the realistic potentials were able to simulate both realistic cooling rates and reproduce the experimentally obtained temperature.

Schwarz [8, 9] developed a Monte-Carlo simulation package to calculate the motion of ions in the presence of arbitrary electric (and/or magnetic) fields and buffer gas. The mobility data K_0 as a function of drift velocity obtained from simulations with a realistic scatting potential were in good agreement with the experimental data [10, 11]. But this is not the case for the simulations with a hard-sphere collision.

We emphasize that all these simulations have been performed for the ions' energies less than 100-200 eV and not beyond. The suitable energy (velocity) range (or energy limitation) is still unknown for these models in the simulation of buffer gas. In this paper we would like to present our results by comparing the stopping ranges of various ions in different buffer gases.

2. Models

2.1. Hard-sphere collision (HSC) model

The HSC model is the simplest approach to handle the cooling force, and it treats the collision between the ion and the buffer gas particle as a collision of hard spheres. The ion travels through the neutral background gas, and collides with those gas particles, which travel in randomized velocities according to the Maxwell-Boltzmann distribution, and then scatters elastically. This approach has been used in a number of calculations and implemented in several simulation packages [7, 12].

2.2. Viscous damping force (VDF) model

Viscous damping is produced by the long-range induced-dipole interaction by which an ion feels the effect of many gas atoms at once rather than the very short range force of a direct collision. The experimental values of ion mobility at low energies enable more accurate simulation of viscous damping than hard-sphere collisions. The validity of VDF model has been verified by the cooling time of ^{39}K in helium gas [6].

If an ion with a charge of q and a mass of m moves in gas, the ion motion is viscously damped, in principle down to the temperature of the gas itself. The time-averaged cooling effect of the buffer gas is often approximated by a viscous drag force. In the simulation, the effect of buffer gas cooling can be explained as ion's acceleration adding a viscous damping acceleration term, which could be express as [6]:

$$\frac{du^2}{dt^2} = \frac{q}{m}\left(-\frac{du}{dt}\frac{1}{K} + \frac{v_{th}}{K_{th}}\right),\tag{1}$$

where u stands for the ion's position, such as x, y and z. K is the ion's mobility, and v_{th} is the thermal velocity of the ion and K_{th} its corresponding mobility. The last term is added to prevent the unrealistic situation in which the ions are cooled to zero temperature since the statistical nature of the collisions of ions with the buffer gas molecules has not been taken into account.

The mobility K value at a given pressure of p and temperature of T can be normalized from the "reduced" value K_0 by

$$K = K_0 \cdot \frac{T}{273.16\,\mathrm{K}} \cdot \frac{1013\,\mathrm{mbar}}{p}.\tag{2}$$

4

Table 1: Fitted parameters for VDF model for different ion/molecule combinations

Ion/Mol	a	b_0	b_1	b_2
Ar^+/He	1.34×10^4	6.29×10^7	-8.21×10^3	0.299
Cs^+/He	2.41×10^4	2.22×10^8	-1.82×10^4	0.395
Hg^+/He	2.70×10^4	2.72×10^8	-1.92×10^4	0.360
Cs^+/Ne	2.83×10^3	1.09×10^7	-5.12×10^3	1.043
Cs^+/Ar	1.58×10^3	8.86×10^6	-3.05×10^3	1.478

K_0 values are known for a wide variety of ions in the low energy part [10, 11, 13]. For the high energy part, they can be approximately calculated from:

$$K_0 \;=\; \frac{2q}{m}\frac{(m+M)^2}{mM} \cdot \frac{1}{N\sigma v}, \tag{3}$$

where M is the mass of the gas particle, N the gas density and σ the cross section for hard-sphere collision.

The whole curve can be easily fitted by the following formula:

$$K_0 \;=\; \frac{v+a}{b_0 + b_1(v+a) + b_2(v+a)^2}. \tag{4}$$

where a, b_0, b_1 and b_2 are fitting parameters. As an example, the reduced mobility K_0 of $^{133}Cs^+$ ion in helium gas is shown in Fig. 1. The data point with velocity lower than 10,000 m/s are taken from Ref. [13] and the others are calculated from Eq. (3). The fitted parameters for different ion-molecule combinations are listed in Table 1.
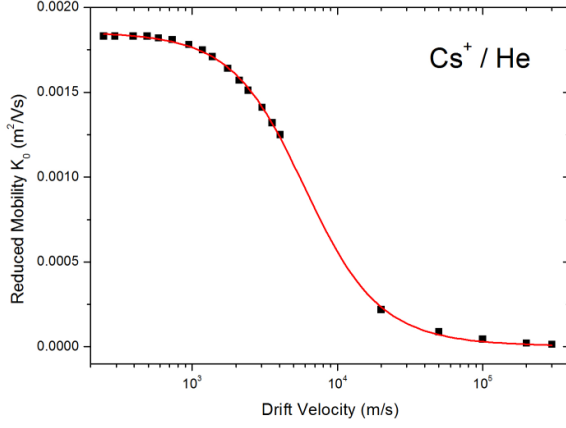
Figure 1: The reduced mobility K_0 of $^{133}Cs^+$ in He-gas versus drift velocity. The data point with velocity lower than 10,000 m/s are taken from Ref. [13] and the others are calculated from Eq. (3). The fitting parameters used: $a = 2.41 \times 10^4$, $b_0 = 2.22 \times 10^8$, $b_1 = -1.82 \times 10^4$, $b_2 = 0.395$.

2.3. Realistic interaction potentials (RIP) model

Although the idea of collisions of hard sphere is quite useful to understand the cooling mechanism, it ignores the long-rang interaction between the ion and the buffer gas particle, which lets the gas act as a viscous medium and lets the ion experience a damping force. The RIP model[1] considers this interaction in a "realistic" way.

The RIP model chooses the potentials $V(r)$ (also called (n,6,4)-potentials) at a distance of r as the sum of one short-range repulsion term and two attractive terms [14],

$$V(r) = \frac{B}{r^n} - \frac{C_6}{r^6} - \frac{C_4}{r^4}. \tag{5}$$

---

[1]The name "Realistic interaction potentials (RIP) model" may be not very appropriate, instead, we may call it n-6-4 model because the (n,6,4)-potentials are used.

6

The C_4/r^4 and C_6/r^6 terms quantify the attractive interaction of the ion's charge with the electric dipole and quadrupole moments, respectively.

Eq. (5) can alteratively be written in the dimensionless form as

$$
\begin{aligned}
V(r) \;\; = \;\; & \frac{n\varepsilon}{n(3+\gamma) - 12(1+\gamma)} \\
& \times \left[\frac{12}{n}(1+\gamma) \left(\frac{r_m}{r} \right)^n - 4\gamma \left(\frac{r_m}{r} \right)^6 \right. \\
& \left. -3(1-\gamma) \left(\frac{r_m}{r} \right)^4 \right],
\end{aligned} \tag{6}
$$

where r_m and ε are the position and depth of the minimum of the potential, respectively, and γ is the dimensionless parameter that measures the strength of the r^{-6} term relative to the r^{-4} term.

The parameters in the potentials (Eq. (5) or (6)) can be derived by fitting the so-called collision integral, a theoretical expression for the collision cross-sections, to experimental data obtained from mobility data [14, 15].

The mobility K can be represented by

$$
K = \frac{3q}{16N} \sqrt{\frac{2\pi}{kT_{eff}} \frac{m+M}{mM}} \frac{1}{\Omega(T_{eff})}, \tag{7}
$$

where q and m are the charge and mass of the ion, respectively, M is the mass of the gas particle, N is the number density of the gas molecules, and k is Boltzmann's constant. The effective temperature T_{eff} accounts for both the gas temperature T_{gas} and the drift velocity v_d of the ion:

$$
\frac{3}{2}kT_{eff} = \frac{3}{2}kT_{gas} + \frac{1}{2}Mv_d^2. \tag{8}
$$

The collision integral (of first order) $\Omega(T)$ is a function of temperature

7

T:

$$\Omega(T) = \frac{4\pi}{(kT)^3} \int_0^\infty \exp\left(-\frac{E}{kT}\right) E^2$$
$$\times \int_0^\infty (1 - \cos(\theta(b,E)))b \, \mathrm{d}b \, \mathrm{d}E. \qquad (9)$$

The deflection angle $\theta(b, E)$ is calculated as a function of the impact parameter b and the relative energy E of the collision:

$$\theta(b,E) = \pi - 2b \int_{r_a}^\infty \frac{1}{\sqrt{1 - \frac{b^2}{r^2} - \frac{V(r)}{E}}} \frac{\mathrm{d}r}{r^2}, \qquad (10)$$

where the distance of closest approach r_a is the outermost root of

$$1 - \frac{b^2}{r_a^2} - \frac{V(r_a)}{E} = 0. \qquad (11)$$

By inserting Eq. (5) or (6) into Eq. (10) and the result into Eq. (7) one obtains a relationship between the sets of potential parameters (n,B,C_6,C_4) or $(n,r_m,\varepsilon,\gamma)$ and the collision integral.

The fitted parameters for the (n,6,4)-potentials for a number of ion-molecule combinations can be found in Ref. [9]. These potentials can also be compared with some high-level *ab initio* calculations. Larry A. Viehland *et al.* [16–20] have performed such calculations to investigate the interactions between the atomic cations and the rare gas particles. They calculated the potential energy curves and compared calculated spectroscopic parameters and transport coefficients with the experimental mobility data. The agreements were excellent. Figure 2 shows the *ab initio* calculated potential energy curves for Cs^+/He and Hg^+/Ar, along with the potentials calculated from Eq. (5) by using parameters in Ref. [9]. As may be seen, in general, the two sets of potential curves are in good agreement, and although the
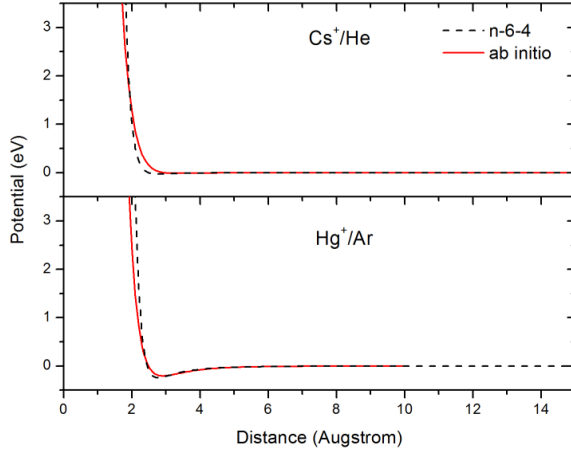
Figure 2: The potential energy curves for Cs^+/He (upper panel) and Hg^+/Ar (lower panel). The black dashed curves represent the potentials calculated from Eq. (5) by using parameters in Ref. [9], while the solid red curves represent the potentials taken from Ref. [21].

curves from the (n,6,4)-potentials change faster than that from the *ab initio* calculations at short ion-molecular separations. Among all the combinations we considered in this paper, the potential curves for Hg^+/Ar combination have the best agreement.

3. Simulations

As the buffer gas cooling is typically used in the ion manipulation in the ion cooler and buncher, such as those in ISOLTRAP [22], SHIPTRAP [23], JYFLTRAP [24, 25], LEBIT [4], CPT [26], LPT [27, 28] and so on, not only the electric (and/or magnetic) fields should be known accurately, but also the effect of the presence of the buffer gas should be modeled adequately. In our

9

simulations, after the electrode layout had been defined, the ion-optics simulation package SIMION [29] was used to obtain the electromagnetic forces acting on the ions. However, for the purpose of this paper, we disabled, i.e. put 0 V on, all the electrodes, thus the movement of the ions is not affected by the presence of electrodes.

To simulate the buffer gas cooling, we used three different models mentioned above: VDF, HSC, and RIP models. In the scheme of the SIMION code, we developed a set of user programs that realized the VDF and HSC models to simulate collisions between the injected ion and the buffer gas. For the RIP model, it is very difficult to do the simulation by using the SIMION, thus we used the "IonCool" code [8], which was developed by Stefan Schwarz, instead. For convenience and comparison the "IonCool" was also used for the HSC model. After detailed simulations, we found that the HSC model results from both the SIMION and the "IonCool" were in good agreement, so we only reported here the results from the SIMION for the HSC model.

For all models, the combinations of three species of ions, relatively light ion - $^{40}Ar^+$, medium ion - $^{133}Cs^+$ and heavy ion - $^{201}Hg^+$, and three buffer gases, He, Ne and Ar, which are often used in the cooler and bunchers, had been simulated. The total number of ions for every simulation was 1,000. The traveling distance of the ion in buffer gas was chosen as the stopping range when the ion's kinetic energy was decreased down to about its thermal energy.

According to the study of Major and Dehmelt [30], only the results for those combinations that the ion's mass is much heavier than the mass of buffer gas particle are reported here, since the cooling effect is our interest.

10

In our calculations, the parameters in Ref. [31], Ref. [9] and in Table 1 have been used for the HSC, RIP and VDF models, respectively.

We used SRIM code [32] for the purpose of comparing the simulation results with the experiments. By using their large collection of stopping power data, Helmut Paul and Andreas Schinner [33] compared those data to various stopping power tables and computer codes to estimate the reliability of these tables and codes. They found that SRIM worked fairly well for all ions and for all energies. Thus we chose the SRIM code to calculate the stopping powers/ranges and then used these calculated values as "experimental" data.

4. Results and analysis

The model differences are illustrated by Fig. 3, as an example, by comparing calculated trajectories based on the VDF, HSC, and RIP models. The chamber is filled with helium buffer gas at a pressure of 1 Pa without the presence of any electric field, and one $^{40}Ar^+$ ion is injected into the chamber along the Z axis with a kinetic energy of 400 eV.

In the simulation by using the VDF model, the ^{40}Ar ion goes along the Z axis and there is no divergence to the X/Y axes (radial direction) except at the very end of the trajectory, and it almost stops at last. This is not the case for the HSC and RIP simulations. The ions go along the Z axis at first, then diverse to the radial direction, and at the end of the trajectories, the ions go randomly and never stop. The reason of this difference lies on whether the collision of ion with the gas particle has been taken into account, i.e., it is not taken into the VDF simulation, but it is in the HSC and RIP simulations.
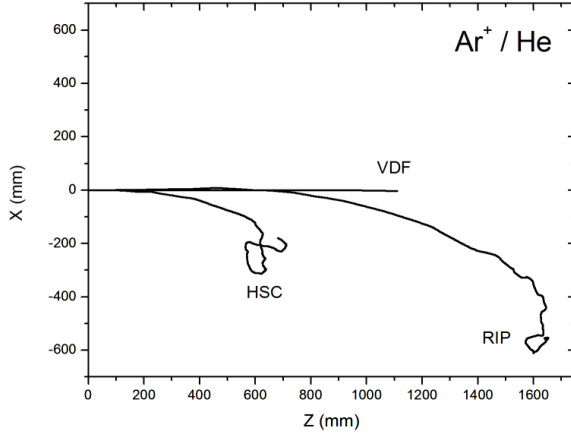
Figure 3: Drift simulation of a single $^{40}Ar^+$ ion in helium buffer gas at a pressure of 1 Pa by using different models. The ion is injected into the chamber, where no any electric field exists, along the Z axis with a kinetic energy of 400 eV. VDF denotes viscous damping force model, HSC hard-sphere collision model, and RIP realistic interaction potentials model.

The corresponding kinetic energies of ^{40}Ar ion versus elapsed time are shown in Fig. 4. It is obvious that the HSC simulation gets the shortest cooling time among all the three simulations, and the RIP the longest. The faster the energy losses, the shorter the cooling time and the smaller the stopping range.

The stopping ranges of Ar^+, Cs^+ and Hg^+ ions in He buffer gas obtained from simulations by using different models mentioned above are shown in the upper panels of Fig. 5. The results from SRIM are also shown for comparison. It is obvious that the VDF and HSC models are better than the RIP model
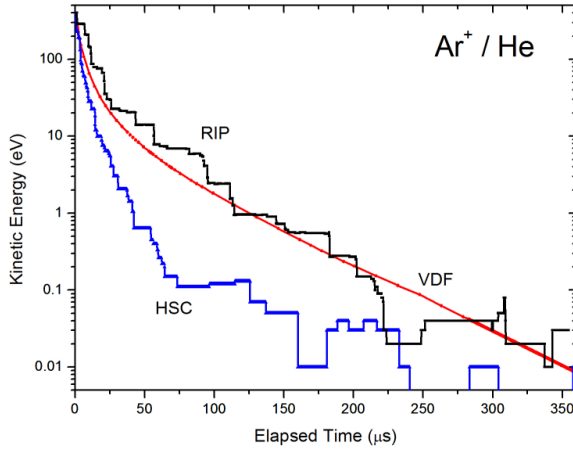
12

Figure 4: The kinetic energy of a $^{40}Ar^+$ ion in helium buffer gas versus elapsed time. See text and Fig. 3.

when the ion's energy is less than ~ 5 eV/u and the stopping ranges agree with the SRIM results better. In the low energy range, the RIP model underestimates the stopping power, i.e., overestimates the stopping range, of the ions in He buffer gas. But in the relatively higher energy range, the RIP model works better than the others. If we only compare the VDF model with the HSC model, we can find that the VDF model is much better. It can be explained by the experimental mobility values, which is only available for low energy ions, used in the VDF model.

For the suitable energy range, generally speaking, in He buffer gas, the VDF model should be used when the ion's energy is less than ~ 5 eV/u, and the RIP model less than ~ 80 eV/u. Above this energy, all three models can not be used and the errors from such simulations are too large.

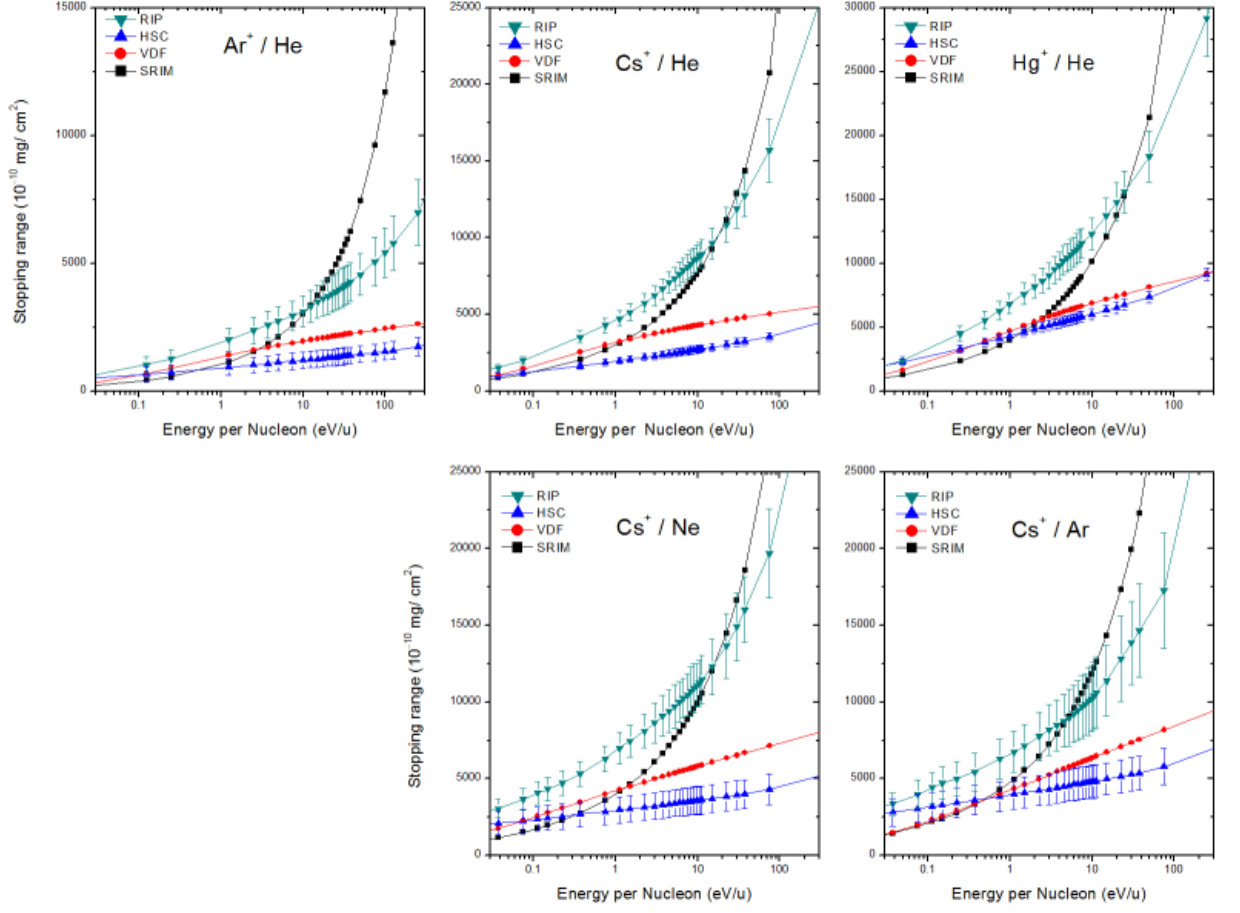Figure 5 shows also the corresponding stopping ranges of Cs$^+$ ion in He-,

Figure 5: The stopping ranges of Ar^+ (upper left), Cs^+ (upper middle) and Hg^+ (upper right) ions in He-gas, and Cs^+ ions in Ne- (lower middle) and Ar-gas (lower right) as a function of ion's energy per nucleon. The error of every data point is the statistical error from the simulation. For the VDF results the error bar is smaller than the symbol size.

Ne-, and Ar-gas obtained from simulations. When the buffer gas becomes heavier, the upper limits to use the models decreases. For the RIP model, this value decreases from ∼80 eV/u in He-gas, to ∼50 eV/u in Ne-gas, and then to ∼20 eV/u in Ar-gas. And for the VDF model, it decreases from ∼5 eV/u in He-gas, to ∼2 eV/u in Ar-gas.

14

5. Conclusions

The VDF, HSC and RIP models to simulate the behavior of ions in buffer gas have been investigated in detail. We found that

- The VDF and HSC models are better in low energy range, but the RIP model is better in relative high energy range.

- In He buffer gas, which is always used in cooler and bunchers nowadays, the VDF model should be used when the ion's energy is less than ~ 5 eV/u, and the RIP model less than ~ 80 eV/u. Above this energy, all three models can not be used.

- If the buffer gas becomes heavier, the upper limits to use the models decrease. For the Cs^+ ion, the upper limit for the RIP model decreases from ~ 80 eV/u in He-gas, to ~ 50 eV/u in Ne-gas, and then to ~ 20 eV/u in Ar-gas. And for the VDF model, it decreases from ~ 5 eV/u in He-gas, to ~ 2 eV/u in Ar-gas.

References

[1] A. Nieminen, J. Huikari, A. Jokinen, J. Äystö, P. Campbell, E.C.A. Cochrane, Nucl. Instr. Meth. A 469 (2001) 244.

[2] F. Herfurth, J. Dilling, A. Kellerbauer, G. Bollen, S. Henry, H.J. Kluge, E. Lamour, D. Lunney, R.B. Moore, C. Scheidenberger, S. Schwarz, G. Sikler and J. Szerypo, Nucl. Instr. Meth. A 469 (2001) 254.

[3] G. Savard, J. Clark, C. Boudreau, F. Buchinger, J.E. Crawford, H. Geissel, J.P. Greene, S. Gulick, A. Heinz, J.K.P. Lee, A. Levand, M. Maier, G. Münzenberg, C. Scheidenberger, D. Seweryniak, K.S. Sharma, G. Sprouse, J. Vaz, J.C. Wang, B.J. Zabransky, Z. Zhou, Nucl. Instrum. Meth. B 204 (2003) 582.

[4] S. Schwarz, G. Bollen, D. Lawton, A. Neudert, R. Ringle, P. Schury, T. Sun, Nucl. Instrum. Meth. B 204 (2003) 474.

[5] M. Block, D. Ackermann, K. Blaum, C. Droese, M. Dworschak, S. Eliseev, T. Fleckenstein, E. Haettner, F. Herfurth, F.P. Heßberger, S. Hofmann, J. Ketelaer, J. Ketter, H.J. Kluge, G. Marx, M. Mazzocco, Y.N. Novikov, W.R. Plaß, A. Popeko, S. Rahaman, D. Rodriguez, C. Scheidenberger, L. Schweikhard, P.G. Thirolf, G.K. Vorobyev, C. Weber, Nature 463 (2010) 785.

[6] M.D. Lunney, R.B. Moore, Int. J. Mass Spectrom. 190/191 (1999) 153.

[7] T. Kim, Buffer gas cooling of ions in an RF ion guide: a study of the cooling process and cooled beam propertiess. Ph.D. Thesis, McGill University, Montreal,1997.

16

[8] S. Schwarz, Nucl. Instr. Meth. A 566 (2006) 233.

[9] S. Schwarz, Lect. Notes Phys. 749 (2008) 97.

[10] H.W. Ellis, R.Y. Pai, and E.W. McDaniel, At. Data Nucl. Data Table 17 (1976) 177.

[11] H.W. Ellis, E.W. McDaniel, D.L. Albritton, L.A. Viehland, S.L. Lin and E.A. Mason, At. Data Nucl. Data Table 22 (1978) 179.

[12] F. Vedel, J. André, M. Vedel, G. Brincourt, Phys. Rev. A 27 (1983) 2321.

[13] L.A. Viehland, E.A. Mason, At. Data Nucl. Data Table, 60 (1995) 37.

[14] E.A. Mason and E.W. McDaniel, Transport Properties of Ions in Gases, Wiley, New York, 1988.

[15] E.W. McDaniel and E.A. Mason, The Mobility and Diffusion of Ions in Gases, Wiley, New York, 1973.

[16] H.L. Hickling, L.A. Viehland, D.T. Shepherd, P. Soldan, E.P.F. Lee, T.G. Wright, Phys. Chem. Chem. Phys. 6 (2004) 4233.

[17] E. Qing, L.A. Viehland, E.P. Lee, T.G. Wright, J. Chem. Phys. 124 (2006) 044316.

[18] T.G. Wright, B.R. Gray, L.A. Viehland, R. Johnsen, J. Chem. Phys. 129 (2008) 184307.

[19] L.A. Viehland, B.R. Gray, T.G. Wright, Mol. Phys. 107 (2009) 2127.

[20] L.A. Viehland, B.R. Gray, T.G. Wright, Mol. Phys. 108 (2010) 547.

[21] VIEHLAND database, http://www.icecat.laplace.univ-tlse.fr.

[22] G. Bollen, S. Becker, H.J. Kluge, M. Konig, R.B. Moore, T. Otto, H. Raimbault-Hartmann, G. Savard, L. Schweikhard, H. Stolzenberg, Nucl. Instr. Meth. A 368 (1996) 675.

[23] G. Sikler, D. Ackermann, F. Attallah, D. Beck, J. Dilling, S.A. Elisseev, H. Geissel, D. Habs, S. Heinz, F. Herfurth, F. Heberger, S. Hofmann, H.J. Kluge, C. Kozhuharov, G. Marx, M. Mukherjee, J. Neumayr, W.R. Pla, W. Quint, S. Rahaman, D. Rodriguez, C. Scheidenberger, M. Tarisien, P. Thirolf, V. Varentsov, C. Weber, Z. Zhou, Nucl. Instrum. Meth. B 204 (2003) 482.

[24] V.S. Kolhinen, T. Eronen, J. Hakala, A. Jokinen, S. Kopecky, S. Rinta-Antila, J. Szerypo, J. Aysto, Nucl. Instrum. Meth. B 204 (2003) 502.

[25] V. Kolhinen, Penning trap for isobaric purification of radioactive beams at IGISOL, PhD thesis, University of Jyväskylä, 2003.

[26] J. Clark, R.C. Barber, C. Boudreau, F. Buchinger, J.E. Crawford, S. Gulick, J.C. Hardy, A. Heinz, J.K.P. Lee, R.B. Moore, G. Savard, D. Seweryniak, K.S. Sharma, G. Sprouse, J. Vaz, J.C. Wang, Z. Zhou, Nucl. Instrum. Meth. B 204 (2003) 487.

[27] W.X. Huang, G.Q. Xiao, Y. Wang, Y.L. Tian, Z.C. Zhu, H.S. Xu, W.L. Zhan, Chin. Phys. C 32 (2008)(S2) 197.

[28] W.X. Huang, Z.C. Zhu, Y.L. Tian, Y. Wang, J.Y. Wang, Y.L. Sun, H.S. Xu, G.Q. Xiao, AIP Conf. Proceedings 1235 (2010) 139.

[29] D.J. Manura, D.A. Dahl, SIMION 8.0 User Manual, Scientific Instrument Services, Inc., Idaho National Laboratory, 2006.

[30] F.G. Major, H.G. Dehmelt, Phys. Rev. 170 (1968) 91.

[31] http://www.webelements.com/atom_sizes.html.

[32] J.F. Ziegler, M.D. Ziegler, J.P. Biersack, Nucl. Instr. Meth. B 268 (2010) 1818.

[33] H. Paul, A. Schinner, Nucl. Instr. Meth. B 209 (2003) 252.